JPET Fast Forward. Published on May 25, 2007 as DOI: 10.1124/jpet.107.121772

JPET #121772

High Dose Acetaminophen Inhibits the Lethal Effect of Doxorubicin in HepG2 Cells: the Role of P-glycoprotein and Mitogen-Activated Protein Kinase p44/42 Pathway.

Irena Manov, Yulia Bashenko, Anat Eliaz-Wolkowicz, Meital Mizrahi,

Oded Liran and Theodore C. Iancu

Pediatric Research and Electron Microscopy Unit, Ruth and Bruce Rappaport Faculty of Medicine, Technion-Israel Institute of Technology, Haifa, Israel

(IM, YB, AEW, MM, OL, TCI)

JPET Fast Forward. Published on May 25, 2007 as DOI: 10.1124/jpet.107.121772
This article has not been copyedited and formatted. The final version may differ from this version.

Running title: Acetaminophen Inhibits Doxorubicin Toxicity in HepG2 cells.

Corresponding author: Irena Manov, Ph.D.

Pediatric Research and Electron Microscopy Unit
Ruth and Bruce Rappaport Faculty of Medicine
Technion-Israel Institute of Technology
P.O. Box 9649, Haifa 31096, Israel
Tel: 972 4 8295367
Fax: 972 4 8295322
E-mail: irmanov@tx.technion.ac.il

Number of Text pages: 30

Number of Tables: 0

Number of Figures: 8

Number of References: 40

Words in Abstract: 247

Words in Introduction: 750

Words in Discussion: 1253

Abbreviations: AAP, acetaminophen; HAAP, high-dose acetaminophen; HCC, hepatocellular carcinoma, DOX, doxorubicin; P-gp, P-glycoprotein; MAPK, mitogen-activated protein kinase; Erk2, extracellular signal-regulated kinase-2; VRP, verapamil; PI, propidium iodide; Rh 123, rhodamine 123; JNK, stress-activated c-Jun N-terminal protein kinase; SEM, scanning electron microscopy; PD98059, 2-(2-amino-3-methoxyphenyl)-4H-1-benzopyran-4-one; NAPQI, N-acetyl-p-benzoquinone imine.

Recommended Section: Chemotherapy, Antibiotics, and Gene Therapy.

JPET Fast Forward. Published on May 25, 2007 as DOI: 10.1124/jpet.107.121772
This article has not been copyedited and formatted. The final version may differ from this version.

Abstract

Doxorubicin (DOX) is a widely used chemotherapeutic drug for human hepatocellular carcinoma (HCC). A major limitation to its effectiveness is the development of multidrug resistance of cancer cells. In clinical trials, patients with advanced HCC were treated with high dose acetaminophen (HAAP) in an effort to improve the antitumor activity of chemotherapeutics. In this study, we investigated the effect of concomitant treatment of DOX and HAAP on hepatoma-derived HepG2 cells. Viability, cell cycle distribution and ultrastructure were examined. Unexpectedly, HAAP, when added to DOX-exposed cells, increased cell viability, released cell cycle arrest and decreased apoptosis. To elucidate the mechanisms by which HAAP reduces the DOX lethal effect to HepG2 cells, we investigated the multidrug resistance P-glycoprotein (P-gp) and p44/42-mitogen-activated protein kinase (MAPK) pathways. The P-gp function was enhanced by DOX and HAAP and was further stimulated during combined treatment leading to decreased DOX retention. Verapamil (VRP), when added to DOX + HAAP exposure, increased DOX accumulation and restored DOX-induced toxicity. The increased phospho-p44/42-MAPK level in DOX-exposed cells was inhibited by HAAP. Additionally, suppression of p44/42 activation by the p44/42-MAPK inhibitor PD98059 blocked DOX-induced apoptosis. These findings suggest that the antagonistic effect of concomitant DOX + HAAP treatment occurs as a result of interactive stimulation of P-gp, generating decreased intracellular drug concentrations. Furthermore, inhibition of the p44/42-MAPK phosphorylation by HAAP could abolish the DOX-induced cell death pathway. Thus, combined treatment by DOX + HAAP, intended to improve chemotherapeutic efficacy, could have an opposite effect facilitating cancer cell survival.

JPET Fast Forward. Published on May 25, 2007 as DOI: 10.1124/jpet.107.121772
This article has not been copyedited and formatted. The final version may differ from this version.

Introduction

Hepatocellular carcinoma (HCC) is a widespread malignancy, hitherto without effective therapy (Coradini and Speranza, 2005). Most patients present in an inoperable stage when chemotherapy is the only alternative. Among the various chemotherapeutics, doxorubicin (adriamycin hydrochloride, DOX) is broadly prescribed to patients with advanced HCC. DOX belongs to anthracyclines antibiotics and its antitumor activity is related to the ability of binding DNA and inhibition of nucleic acid synthesis, leading to apoptosis (Gewirtz, 1999). Unfortunately, repetitive DOX treatment induces multidrug resistance of cancer cells resulting in therapeutic failure (Rittierodt and Harada, 2003; Puhlmann et al., 2005). Novel combination regimens are needed to enhance the efficacy of anthracyclines. Acetaminophen (paracetamol, 4-hydroxyacetanilide, AAP) in high dose (HAAP) rescued by N-acetylcysteine, has been tested for the treatment of advanced HCC and metastatic melanoma (Kobrinsky et al., 1996, 2005; Wolchok et al., 2003). In these trials, HAAP was combined with cisplatin (Kobrinsky et al., 2005) or alkylating agents (Wolchok et al., 2003). It was concluded that chemotherapy combined with HAAP could prolong survival of patients with advanced malignancies.

AAP, a widely used analgesic and antipyretic, is hepatotoxic when given in overdose (Hinson et al., 2004). The mechanisms of AAP hepatotoxicity are well defined and most steps of its molecular pathogenesis have been elucidated (Hinson et al., 2004; Jaeschke and Bajt, 2006). The predominant event of AAP-induced liver toxicity is its transformation by microsomal enzymes of the P450 family, presumably by CYP2E1, into the reactive metabolite N-acetyl-p-benzoquinone imine (NAPQI) which is detoxified by GSH conjugation. Once GSH is depleted, NAPQI stimulates oxidative stress causing liver cell necrosis. The role of apoptotic pathway during AAP

hepatotoxicity remains controversial (Ray and Jena, 2000; Gujral et al., 2002; Jaeschke and Bajt, 2006). Nevertheless, studies of AAP toxicity in hepatoma cell lines, performed in our and other laboratories, unequivocally indicate the occurrence of apoptosis (Boulares et al., 2002, Neuman, 2002; Manov et al., 2002, 2004; Macanas-Pirard et al., 2005; Lee et al., 2006b). Since metabolic activation of AAP is reduced or does not occur in tumor cells, unmetabolized AAP contributes directly to the toxicity, causing apoptosis (Boulares et al., 2004). It was therefore proposed that DOX + HAAP combined chemotherapy may be more effective compared to single-agent treatment. Thus, we investigated the result of DOX and HAAP concomitant treatment using HepG2 cells. These cells, originally derived from HCC (Aden at al., 1979), demonstrate relatively low activities of drug enzymes responsible for AAP metabolic activation (Dai and Cederbaum, 1995). A more recent study revealed a reduced level of CYP2E1 gene expression in HCC, which further decreased during HCC progression (Man et al., 2004). Therefore, usage of HepG2 cells to study of chemotherapeutic efficacy of HAAP and HAAP + DOX seems to be justified and would reflect a clinical situation in which HAAP is administered to HCC patients as an additional anticancer drug. Contrary to our hypothesis, HAAP markedly reduced the lethal effect of DOX to HepG2 cells. Consequently, we investigated the mechanisms which could be involved in the antagonistic effect of combined DOX + HAAP treatment. Specifically, we studied the roles of the multidrug resistance P-glycoprotein (P-gp) and p44/42-mitogen-activated protein kinase (MAPK) pathways in response to DOX, HAAP and in combination.

P-gp belongs to the family of ATP-binding cassette transporters that carries drugs out of the cells (Hoffmann and Kroemer, 2004). Overexpression of P-gp in tumor cells and its up-regulation during chemotherapy decreases intracellular accumulation

of various anticancer drugs, reducing their efficacy (Hoffmann and Kroemer, 2004; Rittierodt and Harada, 2003; Puhlmann et al., 2005). Our previous results indicated that AAP is a P-gp substrate and in high doses increases its function in hepatoma-derived cells (Manov et al., 2006). Hence, the modulation of P-gp by HAAP in cancer cells could influence their chemosensitivity. We therefore investigated whether HAAP can modulate intracellular DOX concentration and DOX-induced damage in HepG2 cells.

Recent studies have indicated a crucial role of p44/42-mitogen-activated protein kinase (MAPK) in DNA damage and apoptosis induced by DOX (Tang et al., 2002; Lee et al., 2006a). Scarce information is available regarding the involvement of p44/42-MAPK pathway in response to HAAP (Macanas-Pirard et al., 2005). Subsequently, we explored p44/42-MAPK activation/suppression during the treatments.

Thus, we aimed to investigate the interaction of DOX and HAAP, using HepG2 cells and to clarify the involvement of P-gp and p44/42-MAPK pathways in the response to the concomitant exposure. We also studied the effects of the P-gp reversing agent verapamil (verapamil hydrochloride, VRP) and of the inhibitor of p44/42 activation PD98059 on the combined or single drug treatment.

Methods

Materials. AAP, DOX, VRP, PD98059 [2-(2-amino-3-methoxyphenyl)-4H-1-benzopyran-4-one], propidium iodide (PI), rhodamine 123 (Rh 123) and dimethyl sulfoxide (DMSO, cell culture grade) were purchased from Sigma-Aldrich Israel Ltd (Rehovot, Israel). Alamar Blue reagent was from Serotec Ltd (Kidlington, Oxford, UK). Polyacrilamide gel-gradient (4–20%) for electrophoresis and enhanced chemiluminescent substrate were from Pierce Biotechnology (Rockford, IL). Cocktail of proteinase inhibitors was from Roche (Indianapolis, IN). Bradford reagent and polyvinylidene difluoride membrane were obtained from BioRad (Hercules, CA). Monoclonal antibody to P-gp (C 219) was from Alexis Biochemicals (San Diego, CA). Anti-β-actin monoclonal antibodies were purchased from Sigma (Rehovot, Israel). Anti- p44/42 and anti-phospho- p44/42 antibody were from Santa Cruz Biotechnology (Santa Cruz, CA). Horseradish peroxidase-conjugated secondary antibody was from Jackson ImmunoResearch Laboratories (West Grove, PA Pierce Biotechnology). Cell culture reagents were from Biological Industries (Kibbutz Beth HaEmek, Israel). All other chemicals, unless otherwise indicated, were obtained from Sigma (Rehovot, Israel).

Cell Culture and Treatments. The HepG2 cell line was kindly provided by Prof. D. Shouval (Liver Unit, Hadassah University Hospital, Jerusalem, Israel). Cells were maintained in RPMI-1640 medium supplemented with 10% FCA and incubated in a humidified incubator at 37ºC in 5 % CO_2. Experiments were initiated when the cells reached 80% confluence. For the experiments, cells were cultured in the FCS-free medium and treated by HAAP (2 and 5 mM), DOX (2 and 5 μM) and HAAP + DOX for 24 and 48 h. To inhibit P-gp function, VRP 50 μM was simultaneously added to drug exposed cells. Pretreatment by the p44/42 MAPK inhibitor PD98059 (30 μM, 2

h) was performed to suppress the p44/42 activation in the cells. HAAP was dissolved in cell culture medium, whereas DOX, VRP and PD98059 were dissolved in DMSO. Final DMSO concentration in culture medium was adjusted to 0.1% in all experiments including vehicle control. In preliminary experiments we confirmed that 0.1% DMSO did not affect survival of HepG2 cells. Alamar Blue reduction test (Nakayama et al., 1997) was used for investigation of cell viability as previously described (Manov et al., 2002).

Cell Cycle Analysis. The cell cycle distribution was assessed by flow cytometry of PI-stained nuclei as described (Manov et al., 2002). In brief, following drug treatment, cells were harvested by trypsin, combined with medium containing floating cells, washed with PBS and stained with hypotonic PI solution (PI 50 μg/ml in 0.1% sodium citrate plus 0.1% Triton X-100). The PI fluorescence of individual nuclei was recorded by using FL2-A histogram plot (cell cycle analysis) and FL2-H for assessment of nuclear hypodiploidity (FACSCalibur, Becton Dickinson, NJ, USA). 20,000 events were acquired and corrected for debris and aggregate population.

Detection of doxorubicin intracellular accumulation. Intracellular DOX accumulation, in the presence or absence of HAAP, was evaluated by using fluorescence microscopy and flow cytometry. Cells were grown on glass coverslips in 6-well tissue culture plates for 48 h and treated by DOX 5 μM with or without HAAP 2 mM for 24 h. After treatment, the cells were washed with PBS and fixed in ice-cold methanol. The coverslips were mounted on glass slides and analyzed with a fluorescent microscope Axioscope2 (Zeiss Inc, Oberkochen, Germany), operated with 546 nm excitation and 590 nm emission filter. For flow cytometry analysis, cells were harvested following the drug treatment (DOX, DOX + HAAP with or without

VRP), washed with PBS and signals generated from intracellular DOX were determined (FL2, 585 nm emission filter).

Measurement of rhodamine 123 retention. Cells were cultured in 6-well plates at a density of 5 x 10^5 cell per well for 48 h, treated by DOX, HAAP or DOX + HAAP with or without the P-gp inhibitor VRP (50 μM) for 24 h prior the addition of Rh 123 (5 μg/ml, 30 min, 37ºC). Thereafter cells were washed with PBS, harvested by 0.05% trypsin with 0.02% EDTA and intracellular Rh-123 fluorescence was estimated by flow cytometry (FL1, 530 nm emission filter). The mean fluorescence intensity and percentage of Rh 123 positive cells were recorded and combined to a fluorescence index (Manov et al., 2006).

Scanning Electron Microscopy (SEM). Cells were grown on glass coverslips in 6-well tissue culture plates and treated by DOX with or without HAAP for 24 h. After treatment, cells were washed with PBS, fixed in 2,5 % glutaraldehyde in 0.1M sodium cacodylate buffer for 1 h, treated with 2% tannic acid + 2% guanidine HCL in PBS for 1 h and post-fixed in 2% OsO_4 (1 h). Thereafter specimens were viewed and photographed using a Jeol J-90 scanning electron microscope, as described (Levanon et al., 2004).

Western blot analysis. Cell lysates, protein determination, electrophoresis and transfer to polyvinylidene difluoride membrane were performed as previously described (Manov et al., 2006). The proteins were probed with the monoclonal antibody to P-gp (C 219, 1:200) or phospho- p44/42 (1:2500), followed by horseradish peroxidase-conjugated secondary antibody and an enhanced chemiluminescent substrate. The levels of β-actin or total p44/42 were measured after stripping of the same membranes and re-probing with anti- β-actin and anti- total

p44/42 (or p42-Erk2) antibody. The optical density of the specific protein bands was quantified by densitometry (Vilber Lourmat, Lyon, France).

Statistical analysis. The data represent the results of at least three separate experiments. Values are the means ± S.D. Statistical differences were analyzed using the Mann-Whitney U test (2-tailed), and $p < 0.05$ was considered statistically significant.

Results

Can HAAP Alter the Sensitivity of HepG2 cells to DOX? To investigate the effect of HAAP on DOX-induced toxicity, we compared viability, cell cycle distribution and ultrastructural changes after exposure of HepG2 cells to DOX, HAAP and DOX + HAAP for 24 and 48 h. The DOX concentrations of 2 and 5 μM used in this study were similar to those reached in the plasma of patients undergoing DOX treatment (Gewirtz, 1999). The AAP concentrations of ~ 2 - 4.5 mM would be achieved in plasma of the patients getting 10–30 g/M^2 of AAP for the treatment of advanced malignancies (Kobrinsky et al., 1996, 2005; Wolchok et al., 2003). In addition, AAP 5 mM has been previously described as the effective dose which caused apoptosis in hepatoma-derived cells (Neuman 2002; Manov et al., 2002, 2004; Macanas-Pirard et al., 2005). Therefore, the concentrations of HAAP 2 and 5 mM and DOX 2 and 5 μM have been used in the present experiments. The changes of cell viability following exposure to HAAP, DOX and in combination are shown in Fig.1. After 24 h of exposure to HAAP 5 mM cell viability decreased ($p < 0.05$ versus vehicle control and HAAP 2 mM). DOX 2 and 5 μM decreased cell viability as well ($p < 0.05$ versus vehicle control). Single-drug treatments for 48 h further reduced cell viability. In opposite, combined treatment by DOX + HAAP increased cell viability when compared with DOX alone. Marked increase of cell viability was observed, after 48 h, when HAAP was added to DOX 2 μM exposed cells.

The cell cycle distributions following the treatment are presented in Fig. 2. DOX 2 μm induced arrest of proliferation mainly in S phase, while Dox 5 μm significantly increased the frequency of apoptotic cells (SubG1). Treatment by HAAP 2 and 5 mM produced a moderate increase in apoptotic cells. HAAP added to DOX-exposed cells, released cell cycle arrest and decreased apoptosis. Ultrastructural changes in the cells

treated by DOX 5 μm, HAAP 2 mM and in combination were investigated by SEM (Fig. 3). Single apoptotic blebs were seen after treatment of HepG2 cells by HAAP 2 mM while prominent apoptotic blebs were present after exposure to DOX 5 μm. These findings disappeared when DOX 5 μM was combined with HAAP.

Does HAAP Reduce DOX intracellular accumulation in HepG2 cells? Figure 4A presents fluorescence microscopic images of cells treated with DOX 5 μM alone and in combination with HAAP 2 mM for 24 h. DOX accumulation visibly decreased when cells were simultaneously treated by HAAP. In parallel, quantitative flow cytometry analysis revealed a significant decrease of DOX fluorescence indices in cells treated by DOX + HAAP in comparison with single DOX exposure (Fig. 4B). The P-gp inhibitor VRP (50 μM), when added to DOX + HAAP treatment, restored DOX intracellular accumulation up to the level reached in DOX + VRP exposure (Fig. 4C).

Is P-gp Involved in the Effect of HAAP on DOX-exposed cells? Our previous observations, performed on HepG2 and Hep3B cells, indicated that HAAP can increase P-gp transport activity (Manov et al., 2006). To investigate whether P-gp is involved in the effect of HAAP on DOX intracellular accumulation and toxicity, we studied the P-gp activity and expression in cells treated by DOX, HAAP and DOX + HAAP (Fig. 5). Measurement of the Rh 123 retention was performed to evaluate the P-gp transport activity in the cells. The fluorescent dye Rh 123 is a substrate for P-gp and its cellular retention has been demonstrated to reflect P-gp function (Petriz and Garcia-Lopez 1997). HAAP decreased the Rh 123 retention in HepG2 cells by a concentration-dependent manner that reflects the increasing P-gp transport activity (Fig. 5A). Single treatment by DOX 5 μM markedly decreased Rh 123 fluorescence as well. Combined treatment with DOX + HAAP resulted in the subsequent decrease

of Rh 123 retention and, respectively, increase of P-gp activity. The stimulation of P-gp activity by HAAP, DOX or DOX + HAAP was fully blocked when the P-gp-reversing agent VRP (50 μM) was added to the cells (Fig 5B). Immunoblots demonstrated the increase of P-gp expression in cells treated by HAAP for 24 h, 1.2 times (2 mM) and 1.7 times (5 mM) in comparison with vehicle control (Fig. 5B). The exposure of cells to DOX alone resulted in a noticeable increase in P-gp content, 2.1 and 3 times at DOX 2 and 5 μM, respectively. Combined treatment with DOX + HAAP did not show a synergistic effect. To evaluate whether VRP can reverse DOX toxicity, we compared cell viability and frequency of hypodiploid (apoptotic) nuclei in HepG2 cells treated by DOX, DOX + HAAP with or without VRP (Fig 6). VRP significantly decreased cell viability and increased nuclear hypodiploidity of DOX + HAAP treated cells, fully restoring DOX toxicity.

Does Inhibition of DOX Toxicity by HAAP Involve p44/42 Dependent Mechanism? Since recent studies have indicated a critical role of p44/42-MAPK pathway in the response to DOX (Lee et al., 2006a; Tang et al., 2002), we explored the p44/42-MAPK cascade during the treatment using immunoblotting (Fig. 7). Exposure of HepG2 cells to HAAP decreased the levels of phospho- p44/42 compared with vehicle control. In contrast, DOX significantly activated the p44/42 pathway by a concentration-dependent manner. When HAAP was added to DOX -exposed cells, p44/42 activation was largely diminished compared with single DOX treatment. The changes in phospho- p44/42 levels after the treatment were observed without modifications in total p44/42. To investigate whether inhibition of p44/42 activity could reduce DOX-induced toxicity, we investigated the effect of p44/42 inhibitor PD98059 on DOX exposure (Fig 8). Pretreatment of HepG2 cells by PD98059 (30 μM, 2h) inhibited DOX toxicity. Cell viability of DOX-exposed cells

pretreated by PD98059 was similar to viability of vehicle control and not different from treatment of PD98059 alone (Fig. 8A). In parallel, DOX-induced nuclear degradation was blocked by PD98059 pretreatment (Fig 8B). Immunoblot with anti-phospho-p44/42 monoclonal antibody confirmed suppression of p44/42 activation in DOX-exposed or vehicle control cells pretreated by PD98059 (Fig. 8C).

Discussion

This study examined the combined effect of DOX and HAAP, using hepatoma-derived HepG2 cells. DOX is one of the most important anticancer drugs for the treatment of solid tumors, including HCC (Hortobagyi, 1997) and has been shown to induce apoptosis via activation of caspases and disruption of mitochondrial membrane potential (Gewirtz, 1999). The significant role of MAPK pathways and p53 activation were described as well (Sanchez-Prieto et al., 2000; Tang et al., 2002; Lee et al., 2006a). Several clinical trials demonstrated the effectiveness of HAAP with N-acetylcysteine rescue for the treatment of patients with advanced HCC and metastatic melanoma (Kobrinsky et al., 1996, 2005; Wolchok et al., 2003). Recently HAAP has been shown to potentiate staurosporine-mediated neuroblastoma cell death (Posadas et al., 2007). Since HAAP causes apoptosis in different tumor cells (Bae at al., 2001; Boulares et al., 2002; Manov et al., 2002, 2004; Macanas-Pirard et al., 2005), we hypothesized that treatment of DOX-exposed HepG2 cells with HAAP would increase tumor cell death. Unpredictably, HAAP strongly reduced the DOX lethal effect to HepG2 cells increasing cell viability, restoring cell cycle and decreasing apoptosis (Figs. 1, 2 and 3). When tested alone, either DOX or HAAP generated reduced viability, growth inhibition and increased apoptosis. To find out the molecular mechanisms playing a role in the antagonistic effect during DOX + HAAP exposure, we investigated the involvement of multidrug resistance P-gp and p44/42 MAPK pathways in the response to DOX, HAAP and co-treatment.

The appearance of drug resistance in tumors is frequently a major obstacle during chemotherapy. Among the transporters, P-gp has been shown to play a central role in the development of multidrug resistance of malignant cells (Hoffmann and Kroemer, 2004). Both P-gp overexpression and its induction by anticancer drugs may generate

cancer cell survival and chemotherapeutic inefficiency. DOX has been shown to increase P-gp function in cancer cells (Rittierodt and Harada, 2003; Puhlmann et al., 2005). We previously reported that HAAP can induce P-gp transport activity and expression in hepatoma-derived cells (Manov et al., 2006). Hence, we hypothesized that P-gp stimulation by HAAP may decrease DOX intracellular accumulation and, consequently, reduce the DOX-induced damage in HepG2 cells. Both DOX and HAAP increased P-gp transport activity and content (Fig. 5 A and C). Combined treatment with DOX + HAAP further stimulated P-gp transport activity resulting in decreased DOX intracellular accumulation (Fig. 4 A and B) and increased Rh 123 efflux (Fig. 5 A). Although P-gp function was induced during combined treatment, no increase of the P-gp expression was observed when compared with single DOX treatment (Fig. 5 C). Furthermore, reduced P-gp bands were found during co-exposure HAAP with DOX 5μM. The most likely explanation of this discrepancy is that HAAP, as P-gp substrate, may induce conformational shift in the C219 binding domain leading to decreased affinity. The finding that P-gp substrates can modulate the P-gp reactivity to bind the specific monoclonal antibody, confirms our suggestion (Druley et al., 2001).

To prove whether stimulation of P-gp contributes to HAAP + DOX antagonism, we studied the effect of the specific inhibitor of P-gp function VRP on DOX accumulation and DOX + HAAP toxicity. If inhibition of DOX toxicity is the result of P-gp activation, VRP would reverse the DOX accumulation and abolish HAAP cytoprotective effect. We have shown that treatment of DOX + HAAP-exposed cells with VRP increased DOX intracellular fluorescence (Fig. 4 C) and fully restored the DOX lethal effect (Fig 6 A and B).

The MAP kinases, which include extracellular-regulated protein kinases (p44/42), the stress-activated c-Jun N-terminal protein kinase (JNK) and p38 kinase, play basic roles in survival, proliferation and apoptosis (Widmann et al., 1999). Little is known about the role of MAPK pathways in HAAP toxicity. It was observed that JNK is activated by HAAP in glioma cells (Bae et al., 2001) and HuH7 cells (Macanas-Pirard et al., 2005), but its pharmacological inhibition did not alter HAAP toxicity. A recent report showed that inhibition of p38 or p44/42 MAP kinases failed to modulate the ability of HAAP to trigger apoptosis in HuH7 cells; therefore the authors concluded that these pathways were not involved in the response to HAAP (Macanas-Pirard et al., 2005). Our results demonstrated that HAAP suppresses the p44/42 pathway in HepG2 cells, as evidenced by the detection of the corresponding phospho p44/42 bands (Fig. 7). The p44/42 kinases have been shown to play a central role in the response to DNA damaging agents such as anthracyclines (Lee et al., 2006a). It was shown that DOX induces the p44/42 pathway in different cell models (Guise et al., 2001; Small et al., 2003; Lee et al., 2006a). Consistent with the previous findings, our results showed that treatment of HepG2 cells with DOX resulted in increased phospho-p44/42 levels (Fig 7). The role of p44/42 activation in the response to DOX remains controversial. Some investigations suggested an anti-apoptotic role of this pathway (Niiya M et al., 2004; Small et al., 2003). For instance, suppression of p44/42 phosphorylation by the inhibitor U0126 was found to increase the caspase-3 cleavage in DOX-exposed RC-K8 lymphoma cells (Niiya M et al., 2004). However, it has not been clearly demonstrated whether the apoptogenic effect is generated via p44/42 inhibition or is due to a direct effect of U0126, which itself markedly enhances the caspase-3 cleavage. Alternatively, suppression of the p44/42 pathway via overexpression of a dominant negative mutant form (Lee et al., 2006a)

or by using antisense strategy (Guise et al., 2001) resulted in decreased DOX toxicity. In our experiments, direct inhibition of p44/42 activity by PD98059 abolished the DOX lethal effect in HepG2 cells (Fig.8). Similar results were obtained in NIH3T3 fibroblasts and SK-N-SH neuroblastoma cells (Tang et al., 2002; Guise et al., 2001). Taken together, these observations suggest that p44/42 activation is the central event in the response to DOX and induction of apoptosis. Therefore, suppression of the p44/42 pathway could attenuate the DOX lethal effect. Indeed, HAAP was able to diminish the p44/42 activation in DOX exposed cells. Thus we suggested that the p44/42 pathway and its inhibition by HAAP could be also involved in the mechanism by which HepG2 cells circumvent the DOX-induced apoptosis.

Our results do not rule out the possibility of other mechanisms playing a role in the DOX + HAAP antagonistic effects. A recent study revealed that AAP stimulates DOX oxidation in human leukemic HL-60 cells that may hinder DOX anticancer activity (Reszka et al., 2004). The authors have shown that GSH protects DOX against its oxidation. When intracellular GSH is depleted by AAP metabolic transformation, DOX undergoes oxidation and turns into a less toxic metabolite. Another possibility is that HAAP, notwithstanding its apoptotic effect to C6 glioma cells, was shown to decrease the level of p53 protein (Lee et al., 2006b). The wild-type p53 is present in HepG2 cells (Lee et al., 2002) and its suppression was found to play a significant role in preventing apoptosis (Sanchez-Prieto et al., 2000; Bai and Cederbaum, 2006). Thus, it may be supposed that p53 inhibition by HAAP could also contribute to this effect. Further studies are required to clarify this hypothesis.

In conclusion, HAAP strongly reduces the lethal effect of DOX on HepG2 cells. This phenomenon occurs due to stimulation of P-gp efflux pump activity by HAAP resulting in decreased DOX intracellular concentration. Furthermore, inhibition of the

p44/42 pathway by HAAP could decrease the response to DOX in cancer cells. We presume that co-administration of DOX and HAAP in attempts to improve the chemotherapeutic efficacy, may have an opposite effect, resulting in cancer cell survival.

Acknowledgments

We thank Mark Hirsh, MD, PhD (Department of Surgery, University of California San Diego School of Medicine, San Diego, CA, USA) for the critical evaluation of the manuscript.

References:

Aden DP, Fogel A, Plotkin S, Damjanov I, and Knowles BB (1979) Controlled synthesis of HBsAg in a differentiated human liver carcinoma-derived cell line. *Nature* **282**: 615-616.

Bae MA, Pie JE, and Song BJ (2001) Acetaminophen induces apoptosis of C6 glioma cells by activating the c-Jun NH(2)-terminal protein kinase-related cell death pathway. *Mol Pharmacol* **60**: 847-856.

Bai J and Cederbaum AI (2006) Cycloheximide protects HepG2 cells from serum withdrawal-induced apoptosis by decreasing p53 and phosphorylated p53 levels. *J Pharmacol Exp Ther* **319**: 1435-1443.

Boulares AH, Zoltoski AJ, Stoica BA, Cuvillier O, and Smulson ME (2002) Acetaminophen induces a caspase-dependent and Bcl-XL sensitive apoptosis in human hepatoma cells and lymphocytes. *Pharmacol Toxicol* **90**: 38-50.

Boulares AH and Ren T (2004) Mechanism of acetaminophen-induced apoptosis in cultured cells: roles of caspase-3, DNA fragmentation factor, and the Ca2+ and Mg2+ endonuclease DNAS1L3.*Basic Clin Pharmacol Toxicol* **94**:19-29.

Coradini D and Speranza A (2005) Histone deacetylase inhibitors for treatment of hepatocellular carcinoma. *Acta Pharmacol Sin* **26**:1025-1033.

Dai Y and Cederbaum AI (1995) Cytotoxicity of acetaminophen in human cytochrome P4502E1- transfected HepG2 cells. *J Pharmacol Exp Ther* **273**:1497-1505.

Druley TE, Stein WD, and Roninson I (2001) Analysis of MDR1 P-glycoprotein conformational changes in permeabilized cells using differential immunoreactivity. *Biochemistry **40*:** 4312-4322.

Gewirtz DA (1999) A critical evaluation of the mechanisms of action proposed for the antitumor effects of the anthracycline antibiotics adriamycin and

daunorubicin. *Biochem Pharmacol* **57**: 727-741.

Guise S, Braguer D, Carles G, Delacourte A, and Briand C (2001) Hyperphosphorylation of tau is mediated by ERK activation during anticancer drug-induced apoptosis in neuroblastoma cells. *J Neurosci Res* **63**: 257-267.

Gujral JS, Knight TR, Farhood A, Bajt ML, and Jaeschke H (2002) Mode of cell death after acetaminophen overdose in mice: apoptosis or oncotic necrosis? *Toxicol Sci* **67**: 322-328.

Hinson JA, Reid AB, McCullough SS, and James LP (2004) Acetaminophen-induced hepatotoxicity: role of metabolic activation, reactive oxygen/nitrogen species, and mitochondrial permeability transition. *Drug Metab Rev* **36**: 805-822.

Hoffmann U and Kroemer H (2004) The ABC transporters MDR1 and MRP2: multiple functions in disposition of xenobiotics and drug resistance. *Drug Metab Rev* **36**: 669-701.

Hortobagyi GN (1997) Anthracyclines in the treatment of cancer. An overview. *Drugs* **4**: 1-7.

Jaeschke and Bajt ML (2006) Intracellular signaling mechanisms of acetaminophen-induced liver cell death. *Toxicol Sci* **89**:31-41.

Kobrinsky NL, Hartfield D, Horner H, Maksymiuk A, Minuk GY, White DF, and Feldstein TJ (1996) Treatment of advanced malignancies with high-dose acetaminophen and N-acetylcysteine rescue. *Cancer Invest* **14**:202-210.

Kobrinsky NL, Sjolander DE, Goldenberg JA, and Ortmeier TC (2005) Successful treatment of doxorubicin and cisplatin resistant hepatoblastoma in a child with Beckwith-Wiedemann syndrome with high dose acetaminophen and N-acetylcysteine rescue. *Pediatr Blood Cancer* **45**: 222-225.

Lee TK, Lau TC, and Ng IO (2002) Doxorubicin-induced apoptosis and

chemosensitivity in hepatoma cell lines. *Cancer Chemother Pharmacol* **49**: 78-86.

Lee ER, Kim JY, Kang YJ, Ahn JY, Kim BW, Choi HY, Jeong MY, and Cho SG (2006 a) Interplay between PI3K/Akt and MAPK signaling pathways in DNA-damaging drug-induced apoptosis. *Biochem Biophys Acta* **1763**: 958-968.

Lee YS, Wan J, Kim BJ, Bae MA, and Song BJ (2006 b) Ubiquitin-dependent degradation of p53 protein despite phosphorylation at its N terminus by acetaminophen. *J Pharmacol Exp Ther* **317**: 202-208.

Levanon D, Manov I, and Iancu TC (2004) Qualitative and quantitative analysis of the effects of acetaminophen and N-acetylcysteine on the surface morphology of Hep3B hepatoma cells in vitro. *Ultrastruct Pathol* **28**: 3-14.

Macanas-Pirard P, Yaacob NS, Lee PC, Holder JC, Hinton RH, and Kass GE (2005) Glycogen synthase kinase-3 mediates acetaminophen-induced apoptosis in human hepatoma cells. *J Pharmacol Exp Ther* **313**:780-789.

Man XB, Tang L, Qiu XH, Yang LQ, Cao HF, Wu MC, and Wang HY (2004) Expression of cytochrome P4502E1 gene in hepatocellular carcinoma. *World J Gastroenterol* **10**:1565-1568.

Manov I, Hirsh M, and Iancu TC (2002) Acetaminophen hepatotoxicity and mechanisms of its protection by N-acetylcysteine: a study of Hep3B cells. *Exp Toxicol Pathol* **53**: 489-500.

Manov I, Hirsh M, and Iancu TC (2004) N-acetylcysteine does not protect HepG2 cells against acetaminophen-induced apoptosis. *Basic Clin Pharmacol Toxicol* **94**: 213-225.

Manov I, Bashenko Y, Hirsh M, and Iancu TC (2006) Involvement of the Multidrug Resistance P-Glycoprotein in Acetaminophen-Induced Toxicity in

Hepatoma-Derived HepG2 and Hep3B Cells. *Basic Clin Pharmacol Toxicol* **99**: 213-224.

Nakayama GR, Caton MC, Nova MP, and Parandoosh Z (1997) Assessment of the Alamar Blue assay for cellular growth and viability in vitro. *J Immunol Methods* **204**: 205-208.

Neuman MG (2002) Synergetic signaling for apoptosis in vitro by ethanol and acetaminophen. *Alcohol* **27**: 89-98.

Niiya M, Niiya K, Shibakura M, Asaumi N, Yoshida C, Shinagawa K, Teshima T, Ishimaru F, Ikeda K, and Tanimoto M (2004) Involvement of ERK1/2 and p38 MAP kinase in doxorubicin-induced uPA expression in human RC-K8 lymphoma and NCI-H69 small cell lung carcinoma cells. *Oncology* **67**: 310-319.

Petriz J and Garcia-Lopez J (1997) Flow cytometric analysis of P-glycoprotein function using rhodamine 123. *Leukemia* **11**: 1124-1130.

Posadas I, Vellecco V, Santos P, Prieto-Lloret J, and Cena V (2007) Acetaminophen potentiates staurosporine-induced death in a human neuroblastoma cell line. *Br J Pharmaco*l **50**:577-585.

Puhlmann U, Ziemann C, Ruedell G, Vorwerk H, Schaefer D, Langebrake C, Schuermann P, Creutzig U, and Reinhardt D (2005) Impact of the cyclooxygenase system on doxorubicin-induced functional multidrug resistance 1 overexpression and doxorubicin sensitivity in acute myeloid leukemic HL-60 cells. *J Pharmacol Exp Ther* **312**: 346-354.

Ray SD and Jena N (2000) A hepatotoxic dose of acetaminophen modulates expression of BCL-2, BCL-X(L), and BCL-X(S) during apoptotic and necrotic death of mouse liver cells in vivo. *Arch Toxicol* **73**: 594-606.

Reszka KJ, Britigan LH, Rasmussen GT, Wagner BA, Burns CP, and Britigan BE

(2004) Acetaminophen stimulates the peroxidative metabolism of anthracyclines. *Arch Biochem Biophys* **427**: 16-29.

Rittierodt M and Harada K (2003) Repetitive doxorubicin treatment of glioblastoma enhances the PGP expression--a special role for endothelial cells. *Exp Toxicol Pathol* **55**: 39-44.

Sanchez-Prieto R, Rojas JM, Taya Y, and Gutkind JS (2000) A role for the p38 mitogen-acitvated protein kinase pathway in the transcriptional activation of p53 on genotoxic stress by chemotherapeutic agents. *Cancer Res* **60**: 2464-2472.

Small GW, Somasundaram S, Moore DT, Shi YY, and Orlowski RZ (2003) Repression of mitogen-activated protein kinase (MAPK) phosphatase-1 by anthracyclines contributes to their antiapoptotic activation of p44/42-MAPK. *J Pharmacol Exp Ther* **307**: 861-869.

Tang D, Wu D, Hirao A, Lahti JM, Liu L, Mazza B, Kidd VJ, Mak TW, and Ingram AJ (2002) ERK activation mediates cell cycle arrest and apoptosis after DNA damage independently of p53. *J Biol Chem* **277**:12710-12717.

Widmann C, Gibson S, Jarpe MB, and Johnson GL (1999). Mitogen-activated protein kinase: conservation of a three-kinase module from yeast to human. *Physiol Rev* **79**:143-180.

Wolchok JD, Williams L, Pinto JT, Fleisher M, Krown SE, Hwu WJ, Livingston PO, Chang C, and Chapman PB (2003) Phase I trial of high dose paracetamol and carmustine in patients with metastatic melanoma. *Melanoma Res* **13**:189-196.

Footnotes

This work was supported by grant I-07-2005 from the Dan David Foundation and by the Milman Fund for Pediatric Research. Dr Manov was supported by the Kamea Fund.

Current address: Pediatric Research and Electron Microscopy Unit, Ruth and Bruce Rappaport Faculty of Medicine, Technion-Israel Institute of Technology, P.O. Box 9649, Haifa 31096, Israel, e-mail: irmanov@tx.technion.ac.il

Legends for figures

Fig. 1. The effect of DOX, HAAP and DOX + HAAP on cell viability of HepG2 cells (Alamar Blue reduction test). Cells were cultured in 96-well plates at a density of 2 $\times 10^4$ cells per well up to sub-confluent monolayer (80%) and treated with DOX (2 and 5 μM), HAAP (2 and 5 mM) or in combination for 24 and 48 hr. After the treatment, 20 μl of Alamar Blue were added per well and incubated at 37ºC for 3 hr. Optical density was measured spectrophotometrically (570 and 630 nm, ELISA plate reader). Cell viability was calculated as percent of the difference between the reductions of Alamar Blue in treated versus control (0.1% DMSO). Results presented as % of controls, mean ± S.D (n = 4). * $p < 0.05$ compared with corresponding concentration of DOX alone; # $p < 0.05$ compared with cells exposed to analogous concentrations of HAAP only. $ $p < 0.05$ comparison between the groups treated by HAAP 2 and 5 mM for the same time period.

Fig. 2. Comparison of cell cycle distributions in the HepG2 cells treated with DOX + HAAP versus cells exposed to DOX or HAAP alone. Cells were cultured in 6-well plates and treated by DOX, HAAP and DOX + HAAP for 48 hr. After treatment, cells were stained by PI as described in *Methods* and fluorescence of individual nuclei was measured by flow cytometry. Data are mean ± S.D. of four experiments (each in triplicate).* $p < 0.05$ comparison between the groups treated by DOX + HAAP and the corresponding concentration of DOX alone. # $p < 0.05$ comparison between the cells exposed to DOX 2 and 5 μM; $ $p < 0.05$ comparison between the groups treated by HAAP 2 and 5 mM .

Fig. 3. Scanning electron microscopy: Cultured HepG2 cells under the effect of DOX and HAAP. (A) Control (0.1% DMSO): cells with preserved borders and without evidence of damage. (B) A few apoptotic blebs (arrows) after exposure to HAAP 2 mM. (C) DOX 5 μM induces appearance of multiple apoptotic blebs (arrows) as well as necrapoptosis (broad arrow). (D) HAAP 2 mM abolishes the damaging effect of DOX: the cells are similar to vehicle control. Original magnification x 1500.

Fig. 4. The effect of HAAP on DOX intracellular accumulation in HepG2 cells and its inhibition by VRP. (A) Fluorescence microscopic images of cells treated with DOX 5 μM alone and in combination with HAAP 2 mM for 24 h. Cells were grown on glass coverslips, treated by DOX 5 μM with or without HAAP 2 mM for 24 h. DOX fluorescence was visualized by using fluorescent microscopy as described in *Methods*. (B) Flow cytometry analysis of DOX fluorescence in cells exposed to DOX (2 and 5 μM) with or without HAAP (2 and 5 mM) for 24 h. Results presented as DOX fluorescence index (mean of fluorescence intensity × % of DOX positive cells / 100). Mean ± S.D (n = 4). * $p < 0.05$ comparison between cells treated with DOX + HAAP and corresponding concentration of DOX alone.
$ $p < 0.05$ comparison between the treatments of DOX 2 and 5μM. (C) The histogram shows DOX fluorescence intensity in HepG2 cells treated by DOX 5 μM and DOX 5 μM + HAAP 2 mM for 24 h in presence or without VRP (50 μM). The DOX fluorescence intensities were recorded by flow cytometry (the histogram depicts one representative result of three independent experiments).

Fig. 5. The effect of DOX, HAAP and DOX + HAAP on the P-gp function and expression in HepG2 cells. (A) P-gp transport function was evaluated by the measurement of retained Rh 123 intracellular fluorescence. Cells were treated with DOX 5 μM, HAAP 2 and 5 mM and in combination for 24 h. After treatment, Rh 123 (5 μg/ml) was added to the cells for 30 min and retained Rh 123 fluorescence was measured by flow cytometry according to *Methods.* Results presented as Rh 123 fluorescence index (mean of fluorescence intensity × % of Rh 123 positive cells / 100). Mean ± S.D (n = 3). * $p < 0.05$ compared with vehicle control; # $p < 0.05$, comparison between cells treated with DOX + HAAP versus treatment by DOX alone; $ $p < 0.05$ comparison between the treatments of HAAP 2 and 5mM. (B) Flow cytometry histogram shows effect of VRP (50 μM) on retained Rh 123 fluorescence in HepG2 cells after 24 h of exposure to DOX 5 μM and DOX 5 μM + HAAP 2 mM (one representative experiment of two is presented).

(C) Western blot analysis of P-gp expression in cell lysates from HepG2 cells exposed to DOX, HAAP and DOX + HAAP. Cell extracts (25 μg of total protein) were electrophoresed, transferred and immunoblotted with monoclonal antibody to P-glycoprotein (C219, 1:200). β-actin was detected using anti-actin antibody, in order to verify equal protein loading. The analysis was repeated three times with protein extract from separate cell lysates. Representative western blot is shown. Mean density ± S.D. # $p < 0.05$, compared with DMSO vehicle control; * $p < 0.05$, comparison between cells treated with DOX + HAAP versus treatment by analogous concentration of DOX alone.

Fig. 6. VRP neutralizes the cytoprotective effect of HAAP in DOX exposed HepG2 cells. Cell viability (A) and frequency of hypodiploid (apoptotic) nuclei (B) were compared in cells exposed to 5 μM DOX + 2 mM HAAP in presence or without of VRP (50 μM) for 24 h. Cell viability was measured by the Alamar Blue reduction test, whereas nuclear hypodiploidy was assessed by flow cytometry (PI staining) as described in *Methods*. Mean ± S.D of three independent experiments. * $p < 0.05$, comparison between the cells treated by DOX + HAAP with VRP and DOX + HAAP without VRP; # $p < 0.05$, comparison between cells treated with DOX + HAAP versus treatment by DOX alone.

Fig. 7. Comparison of phospho- p44/42 in cells exposed to DOX, HAAP and DOX + HAAP. HepG2 cells were exposed to DOX 2 and 5 μM, HAAP 2 and 5 mM and in combination for 24 h, and analyzed by western blotting. Cell extracts (64 μg of total protein) were electrophoresed, transferred and immunoblotted with monoclonal antibody to p44/42 (1:2500). Loading controls were carried out by re-probing the blots for total cellular p44/42. One representative western blot from three separate experiments is shown. Mean density ± S.D. # $p < 0.05$, compared with vehicle control (0.1% DMSO); * $p < 0.05$, comparison between the cells treated with DOX + HAAP versus treatment by equivalent concentration of DOX alone.

Fig 8. The effect of the p44/42 inhibitor PD98059 on DOX-induced toxicity in HepG2 cells. Cells were pretreated with PD98059 (PD, 30 μM, 2h in FCS-free RPMI) and subsequently incubated with 5 μM DOX or 0.1% DMSO (control) for 24 h. Cell viability (A) was measured by the Alamar Blue reduction test and frequency of hypodiploid (apoptotic) nuclei (B) was investigated by flow cytometry

of PI stained nuclei as described in *Methods*. Mean ± S.D of three independent experiments. * $p < 0.05$ compared with DOX alone; # $p < 0.05$ compared with vehicle control; $ $p < 0.05$ compared with PD98059 alone. (C) Western blot analysis shows the levels of phospho-p44/42 in vehicle control (RPMI contained 0.1% DMSO), DOX treatment (5 μM, 24 h), PD98059 (PD 30μM for 2 h, then RPMI with 0.1% DMSO for 24 h) and PD98059 + DOX (PD 30μM 2 h, then DOX 5 μM for 24 h). Cell extracts (35 μg of total protein) were electrophoresed, transferred and immunoblotted with monoclonal antibody to p44/42 (1:2500). Equal loading was confirmed by re-probing with antibodies that recognized non-phosphorylated p42 (Erk2). One representative result of two is shown.

JPET Fast Forward. Published on May 25, 2007 as DOI: 10.1124/jpet.107.121772
This article has not been copyedited and formatted. The final version may differ from this version.

Figure 1

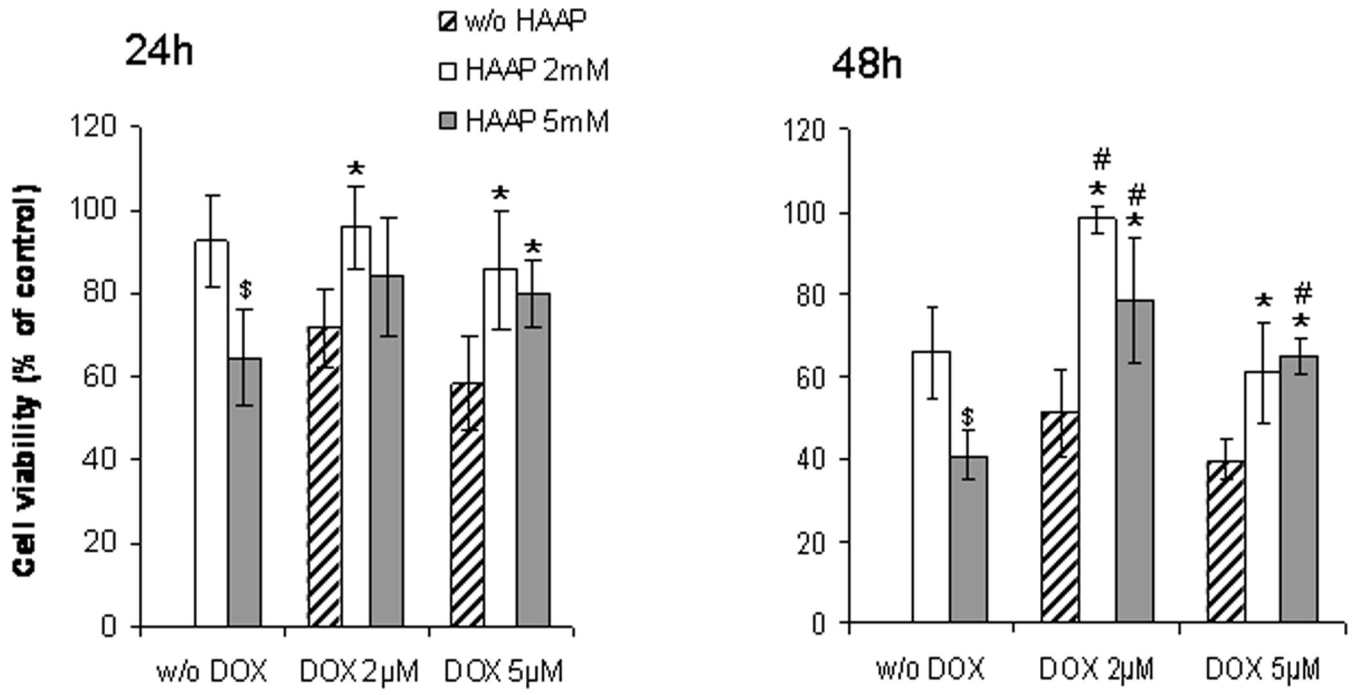

JPET Fast Forward. Published on May 25, 2007 as DOI: 10.1124/jpet.107.121772
This article has not been copyedited and formatted. The final version may differ from this version.

Figure 2

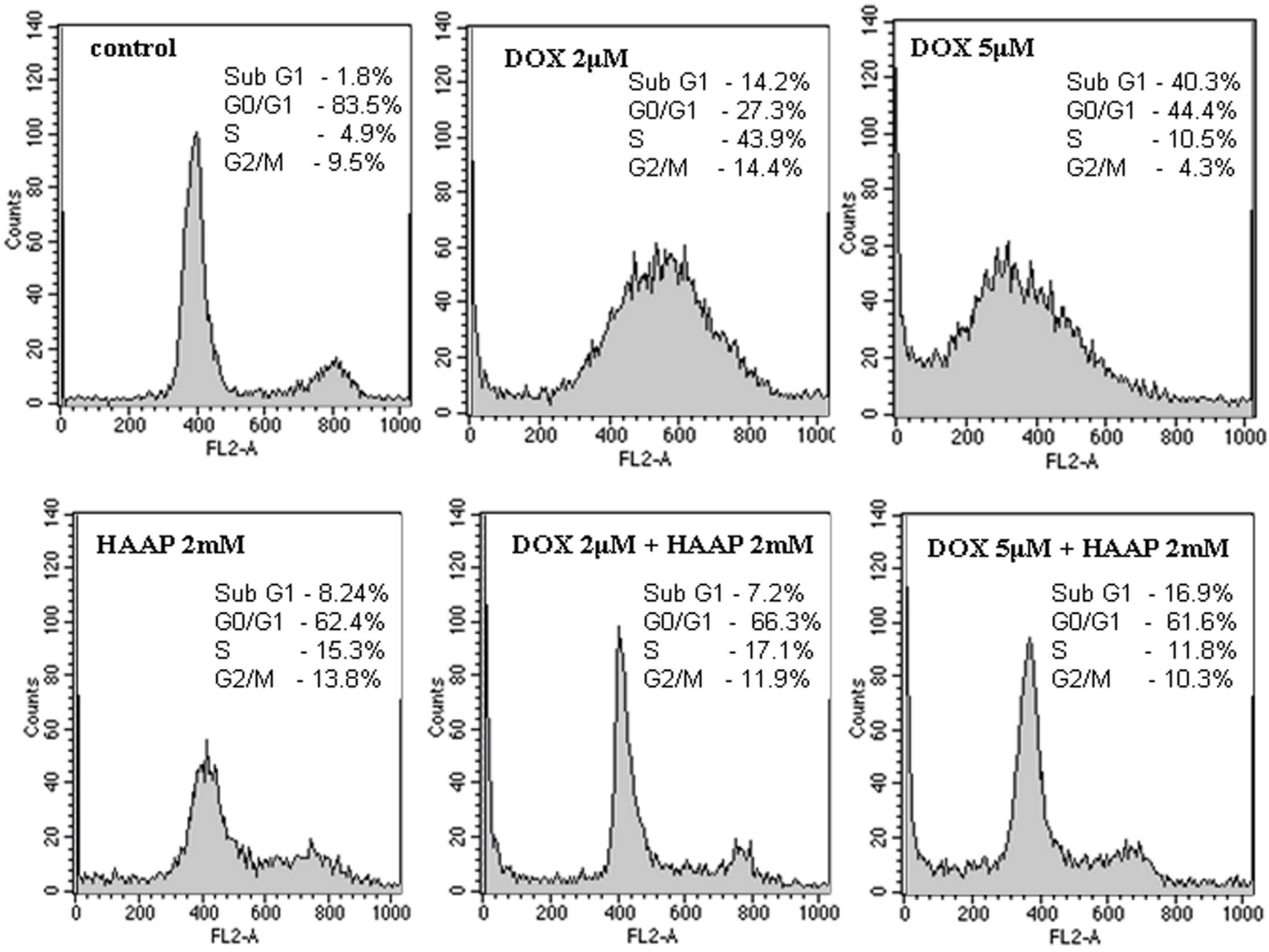

Treatment	Cell Cycle Distribution (%) Sub-G1	G0/G1	S	G2/M
Control	1.8 ± 0.5	79.2 ± 2.6	7.5 ± 1.8	11.1 ± 1.7
HAAP 2 mM	8.6 ± 3.5	65.4 ± 3.5	14.8 ± 3.1	10.7 ± 2.6
HAAP 5 mM	14.6 ± 3.1$	58.8 ± 1.4	17.2 ± 3.5	9.3 ± 1.9
DOX 2µM	11.1 ± 2.6	35.2 ± 7.7	40.7 ± 5.2	12.9 ± 2.0
DOX 5µM	35.6 ± 7.5#	42.4 ± 5.8	16.8 ± 6.4#	4.6 ± 0.4#
DOX 2 µM + HAAP 2 mM	6.9 ± 1.7*	67.4 ± 1.5	15.1 ± 1.8*	10.3 ± 1.5
DOX 2 µM + HAAP 5 mM	9.0 ± 0.8	66.6 ± 1.0	13.8 ± 1.9*	10.1 ± 1.8
DOX 5 µM + HAAP 2 mM	16.5 ± 0.7*	62.8 ± 1.8	11.0 ± 1.2	9.1 ± 0.4
DOX 5 µM + HAAP 5 mM	19.3 ± 4.2*	58.5 ± 3.4	11.9 ± 0.3	9.9 ± 0.7

JPET Fast Forward. Published on May 25, 2007 as DOI: 10.1124/jpet.107.121772
This article has not been copyedited and formatted. The final version may differ from this version.

Figure 3

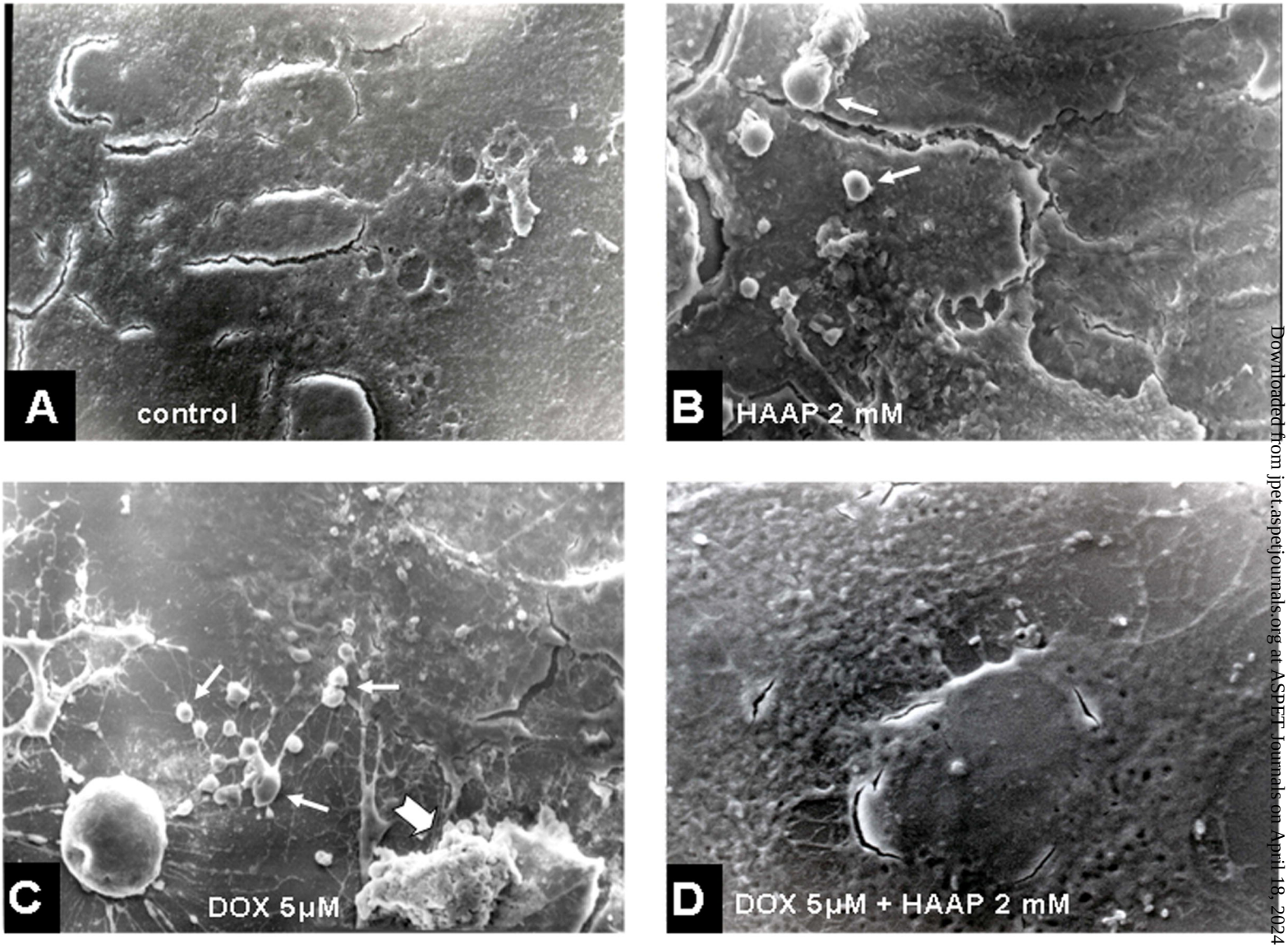

JPET Fast Forward. Published on May 25, 2007 as DOI: 10.1124/jpet.107.121772
This article has not been copyedited and formatted. The final version may differ from this version.

Figure 4

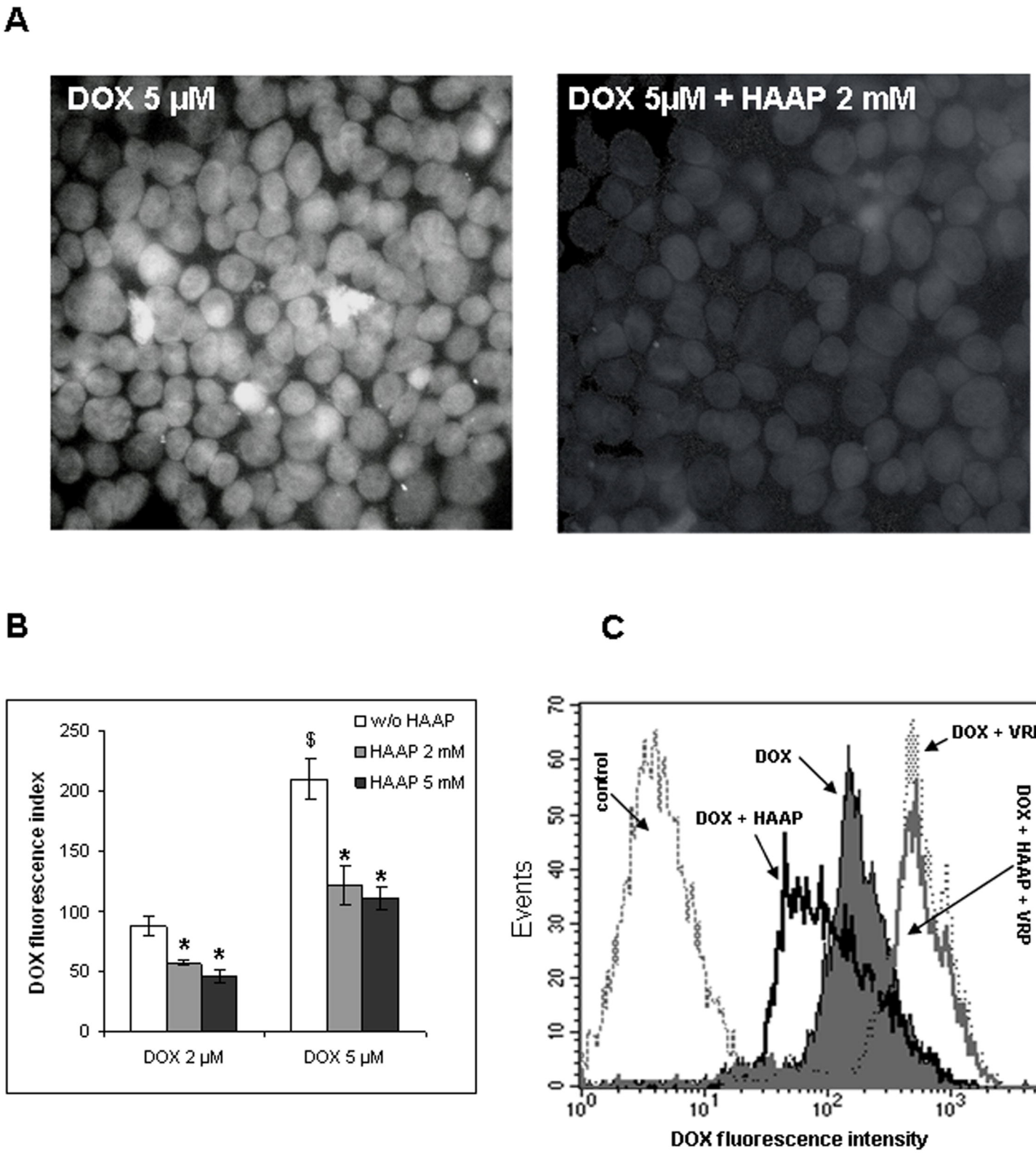

JPET Fast Forward. Published on May 25, 2007 as DOI: 10.1124/jpet.107.121772
This article has not been copyedited and formatted. The final version may differ from this version.

Figure 5

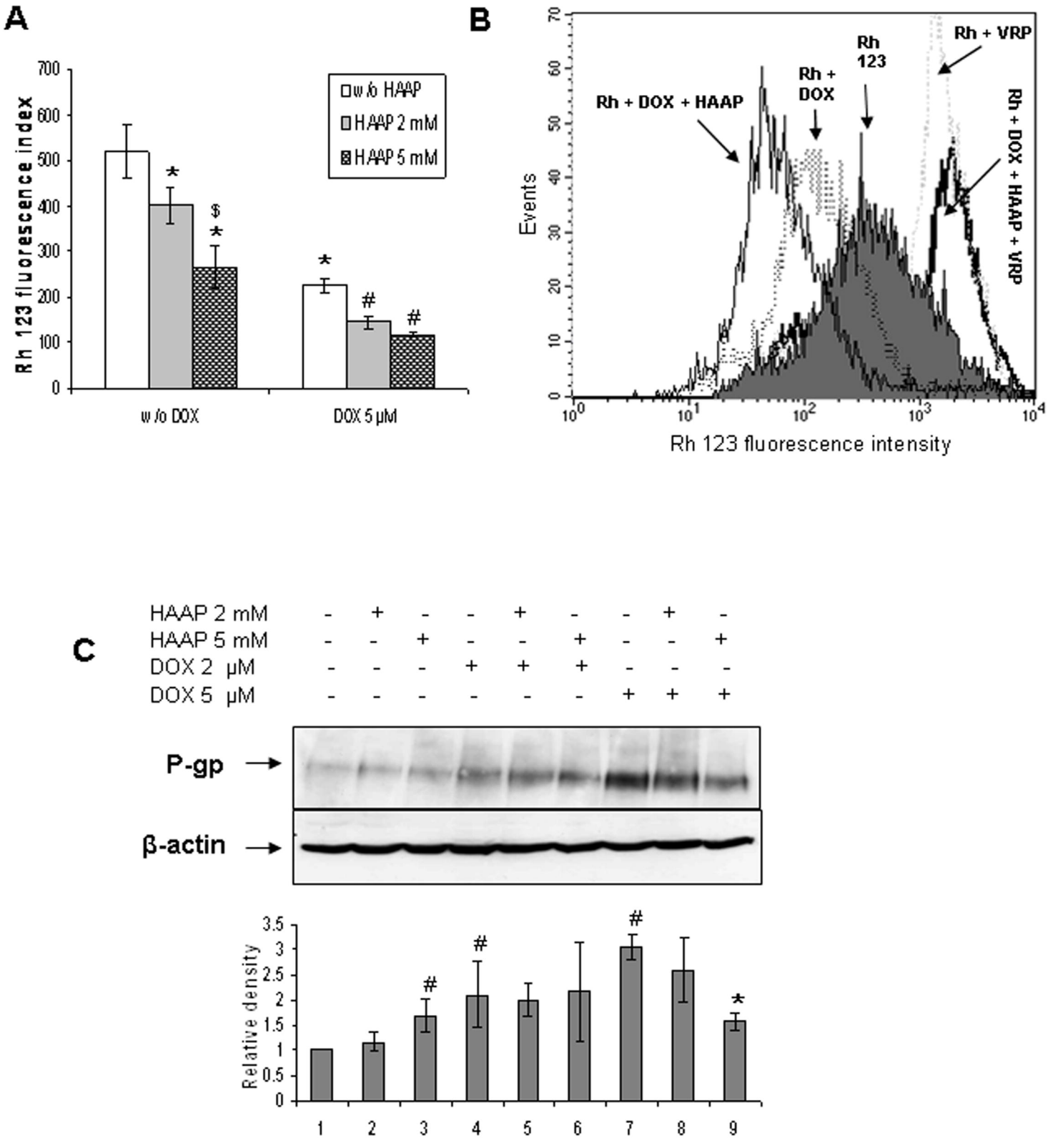

JPET Fast Forward. Published on May 25, 2007 as DOI: 10.1124/jpet.107.121772
This article has not been copyedited and formatted. The final version may differ from this version.

Figure 6

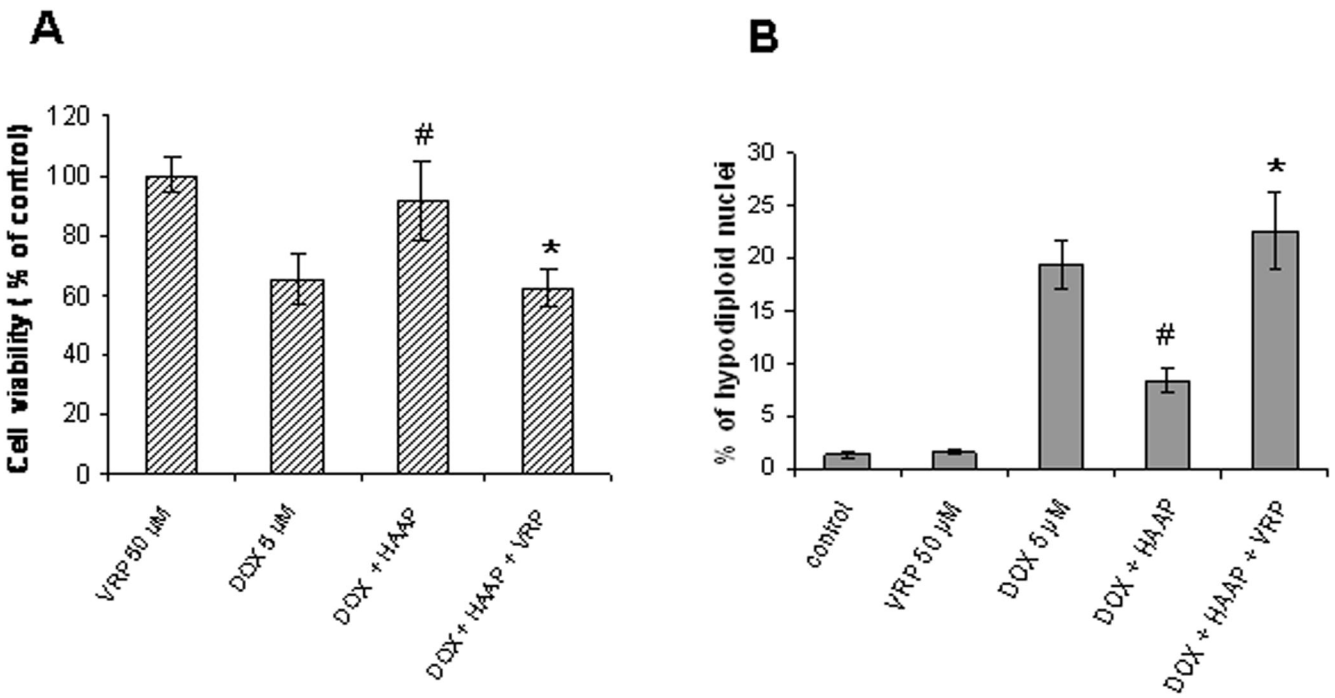

JPET Fast Forward. Published on May 25, 2007 as DOI: 10.1124/jpet.107.121772
This article has not been copyedited and formatted. The final version may differ from this version.

Figure 7

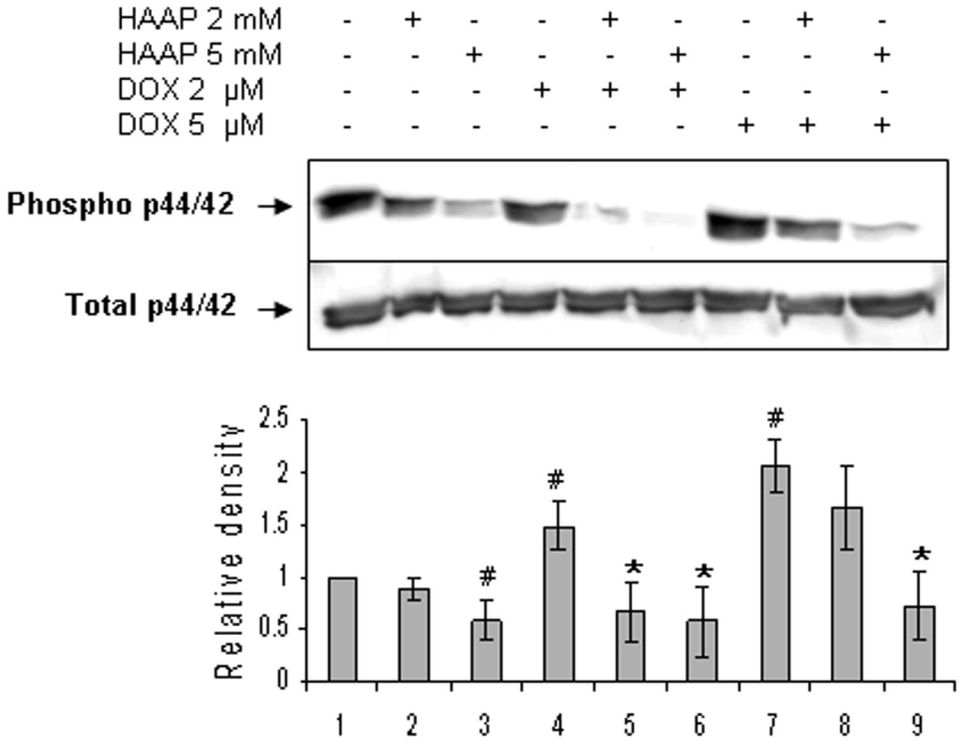

JPET Fast Forward. Published on May 25, 2007 as DOI: 10.1124/jpet.107.121772
This article has not been copyedited and formatted. The final version may differ from this version.

Figure 8